Journal of Applied Electrochemistry **30**: 717–722, 2000.

Effect of heat treatment on the anodic oxidation of Ti–0.2 Pd alloys in chloride solutions

P.L. CABOT[1], A. FORN[2], M. VILARRASA[1], J.A. PICAS[2], F.J. GIL[2] and J.M. COSTA[1]
[1]*Departament de Química Física, Universitat de Barcelona, Barcelona, Spain*
[2]*Departament de Ciència dels Materials i Enginyeria Metal.lúrgica, Universitat Politècnica de Catalunya, Vilanova i la Geltrú, Spain*

Received 28 April 1999; accepted in revised form 9 November 1999

Key words: anodic oxidation, chloride solutions, heat treatments, pitting corrosion, Ti–0.2 Pd alloys

Abstract

The effect of heat treatment of Ti and Ti–0.2 Pd alloys on their anodic oxidation was studied in deaerated 1% NaCl by means of anodic linear sweep voltammetry, SEM, TEM, EDS, optical microscopy and microhardness measurements. The specimens, as fabricated, consisted of α-phase only. The β-phase, intergranular or with a Widmansttäten type growth, was produced by heat treatment of the Ti–0.2 Pd alloys at the temperature range from 750 to 850 °C. The β-phase was transformed into the α'-phase during quenching. The current density against voltage curves for pure Ti and Ti–0.2 Pd, as fabricated or heat-treated, presented an initial plateau at about 1.5 V vs Ag/AgCl/KCl (3 M), an anodic peak at about 4.5 V and a current increase due to the pitting attack at about 10 V. The anodic peak was related to an oxide growth together with a solution electrolysis. Current spikes appeared at random from potentials about 8.3 V, which were related to film breakdown and repair events. The passive films of the alloys oxidized up to about 10 V presented oxidation bands parallel to the surface, with different oxygen content and microhardness, together with a structural transformation of the α'-phase under the titanium oxide layer. The similar behaviour of pure Ti and Ti–0.2 Pd alloys in front of pitting corrosion in chloride was due to such a structural transformation.

1. Introduction

Titanium and titanium alloys are corrosion resistant materials which may be applied in mechanical engineering and chemical apparatus construction [1]. There is also renewed interest in using Ti in marine environments [2]. Its electrochemical stability is due to the spontaneous formation of a thin TiO_2 film, about 2 nm thick in the native state, on the metal surface. Pitting in halide solutions occurs at potentials depending on the anion [3–14]. The breakdown potential of the TiO_2 film is significantly lower in Br^- than in Cl^- and also than in I^-. Breakdown potentials lower than 5 V have been reported for Br^-, whereas those found for Cl^- are higher than about 10 V. The breakdown potential has also been shown to depend on the oxide thickness. Pitting by Br^- was related to the electrical conductivity of particular regions and to the defect structures in the oxide film [3].

Titanium and some titanium alloys are biocompatible materials which find application as biomaterials [7–11]. Commercially pure grade Ti and Ti–6 Al–4 V alloy have both been employed in implantable devices for several decades. However, despite its corrosion resistance, considerable controversy has developed over its biocompatibility [7–10]. The mixed phase α–β alloys Ti–6 Al–4 V and Ti–6 Al–7 Nb presented the best combination of both corrosion and wear resistance, although Ti–Pd [15, 16] and the near-β Ti–13 Nb–13 Zr and β Ti–15 Mo alloys displayed the best corrosion resistant properties [12].

Pure Ti presents an allotropic transformation at 882.5 °C, from a close-packed hexagonal crystal structure (α-phase) to a body-centred cubic one (β-phase) [17]. Different alloying elements can vary such a transformation temperature [14, 18–21]. The Ti–Pd system presents an $\alpha \leftrightarrow \beta$ temperature transition range which seems to start at about 750 °C. A quenching from these or higher temperatures produces a transformation of the β-phase into the martensitic α'-phase, which shows a hexagonal structure similar to that of the α-phase.

It is generally accepted that commercially pure Ti and single phase Ti alloys show the best corrosion resistance. However, heat treated alloys with both α and β-phases have better mechanical properties than those with only one of these phases [20, 21]. Palladium is β-stabilizing and presents a low solubility in the α-phase. The Ti–Pd system presents an eutectoid reaction ($\beta \rightarrow \alpha + Ti_2Pd$) for a Pd composition of 10 at % and a temperature of

595 °C [17, 22]. The formation of Ti_2Pd by the eutectoid reaction has to be avoided because the intermetallic compound produces the alloy embrittlement. The addition of small amounts of Pd increases the corrosion resistance of Ti [15, 16, 23]. The addition of Pd increases the exchange current density of Ti and therefore, facilitates passivation in many systems [23]. Ti–0.2 Pd are considered promising materials for the manufacture of high-level nuclear waste containers [1].

In this work, different heat treatments have been applied to pure Ti and Ti–0.2 Pd alloy in order to study the corresponding microstructures and their effect on the anodic oxidation in chloride solutions. The techniques employed were linear sweep voltammetry, SEM, TEM, EDS, optical microscopy and microhardness measurements.

2. Experimental method

2.1. *Materials*

Commercially pure Ti and Ti–Pd alloy containing 0.2 wt % Pd were prepared as plates 1.5 mm thick, rolled, annealed at 675 °C and cooled in air (IMI Titanium Ltd, England). The results of the chemical analysis are listed in Table 1. These plates were heat treated for 2 h at constant temperature in a tubular furnace in the presence of an argon atmosphere to avoid the oxidation of the specimens. Pure Ti plates were heat treated at 1000 °C whereas different Ti–0.2 Pd alloy plates were heat treated at 750, 800, 850 and 1000 °C. After the heat treatment, the specimens were quenched in water at room temperature. According to the corresponding phase equilibrium diagram [17, 22], an allotropic transformation from the α-phase to the β-phase takes place for the Ti–0.2 Pd alloy in the temperature range from 750 to 900 °C.

2.2. *Anodic oxidation tests*

The electrochemical experiments were performed in a conventional three-electrode cell using a 1287 Solartron potentiostat/galvanostat and the CorrWare for Windows Electrochemistry/Corrosion software (version 1.2). The working electrodes were discs 6 mm in diameter, cut from the Ti and Ti–Pd plates with a shearing die. A copper wire was cold-welded to one side of the disc, opposite to the electrolyte, and embedded in epoxy resin. Prior to the experiments, the disc was polished to 1 μm finish using diamond paste and ethanol in ultrasonic bath to remove the smut. A Pt wire was used as auxiliary electrode. The reference electrode was Ag/AgCl/KCl (3 mol dm^{-3}). All the potentials given in this work are referred to the latter. The electrochemical tests were performed in deaerated and quiescent 1% NaCl at 25 °C. The electrolyte was deaerated by argon sparging with stirring, and during the measurements, argon was passed over the solution. The open circuit potential (OCP) of the working electrodes were measured with time. Linear sweep voltammograms at 0.2 and 0.5 mV s^{-1}, from the quasistationary OCP to different anodic limits, were obtained.

Table 1. Composition of pure Ti and Ti–0.2 Pd (wt %)

Material	Pd	Fe	O	N	C	H
Ti	–	0.035	0.05	0.05	0.10	0.001
Ti–0.2 Pd	0.17	0.05	0.15	0.007	< 0.08	0.01

2.3. *Microscopic analyses*

The specimens were characterized by optical microscopy, TEM (JEM-1200EX II Jeol), SEM (JSM-6400 Jeol) and EDS (Link Analytical LZ-5). The metallographic characterization was performed on small pieces of the plates, embedded in epoxy resin, polished to 1 μm finish as indicated above and etched, for approximately 1 min, with a solution containing both HF (5%) and HNO_3 (35%). For the TEM observations, the samples were reduced in thickness by electrolytic polishing (Tenupol 2) with a solution containing 2-butoxiethanol, perchloric acid and methanol. The process was carried out with a voltage of 25 V and a temperature of −20 °C. After the electrochemical polarizations, sections of different samples were cut in order to be observed under the microscopes and to characterize the effect of the process. Microhardness measurements were also performed for characterization using a Shimadzu tester.

3. Results and discussion

The different microstructures of the Ti–0.2 Pd alloys, as fabricated and also submitted to the heat treatments mentioned above are shown in Figure 1(a)–(e). The microstructure of the alloy before the application of any heat treatments was that exemplified in Figure 1(a), where the equiaxial grains of phase α can be seen. This was also the structure of pure Ti. The micrographs corresponding to the microstructures produced on the Ti–0.2 Pd alloy by the heat treatments at 750, 850 and 1000 °C are shown in Figure 1(b), (c) and (e), respectively. At 750 and 800 °C, the β-phase is formed in the grain bodies and presents an acicular form (Figure 1(b)). This corresponds to a Widmanstätten-type growth. A careful examination under the SEM showed that the needle-like structures appearing in Figure 1(b) were cavities. The β-phase was present in these cavities at the heat treatment temperature. However, it was transformed into the martensitic phase (α') during quenching, and the martensitic phase appears to be easily dissolved in the reagent to reveal the microstructure.

Heat treatment at 850 °C of the Ti–0.2 Pd alloy produces a rapid nucleation of the β-phase in the grain boundaries (Figure 1(c)). As demonstrated by the TEM

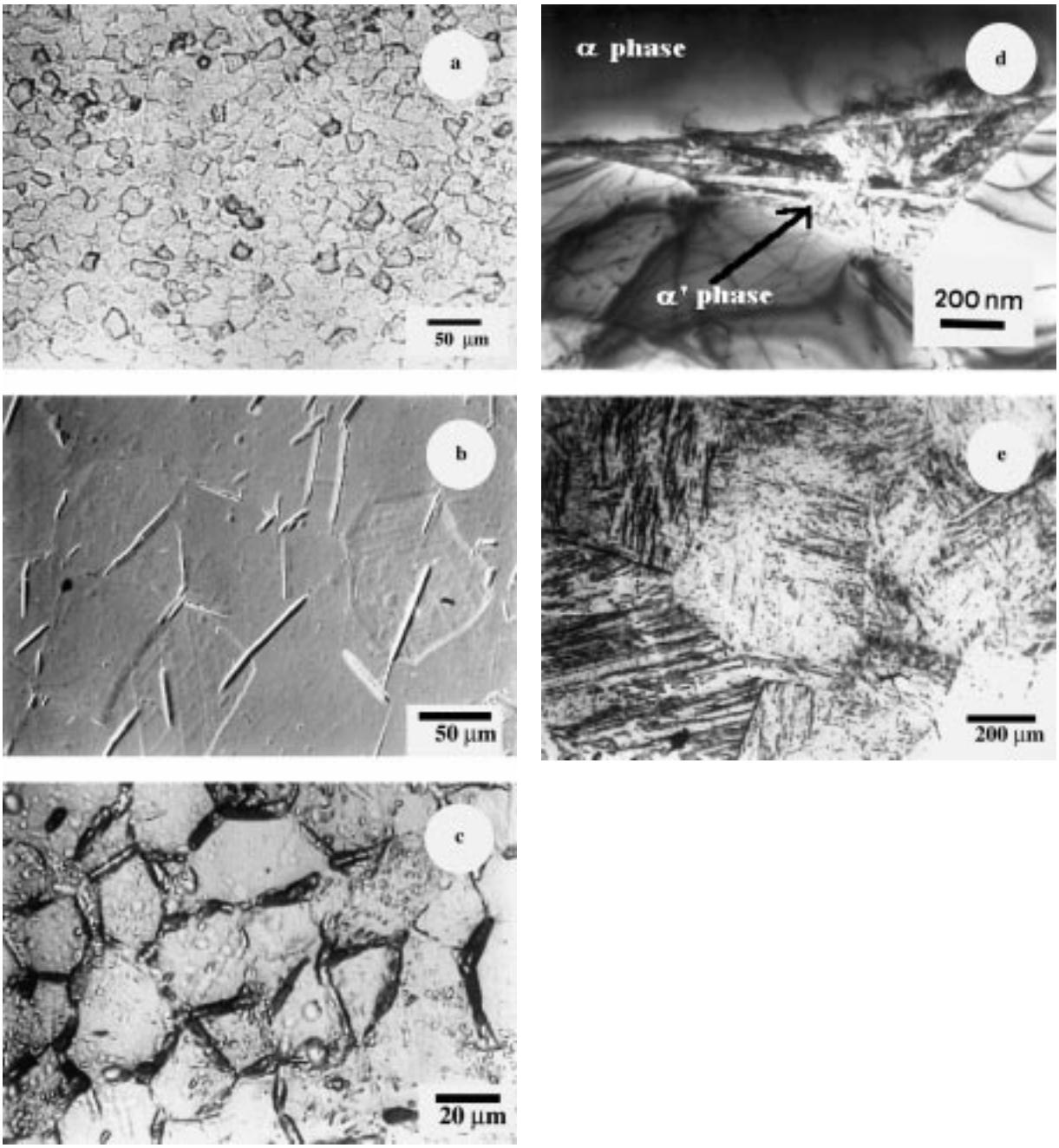

Fig. 1. Micrographs of the Ti–0.2 Pd alloy showing the effect of different heat treatments. (a) Optical microscopy image in the absence of any heat treatments. (b) SEM image, heat treatment at 750 °C. (c) Optical microscopy image, heat treatment at 850 °C. (d) TEM image corresponding to the sample of Figure 1(c) (dark field). (e) Optical microscopy image, heat treatment at 1000 °C. The samples of Figures (a), (b), (c) and (e) were etched as indicated in the experimental part.

micrograph shown in Figure 1(d), this phase is also transformed into the martensitic phase during quenching. The structure of the martensitic phase takes the form of crossed plates, and this form is also found in the optical micrograph of Figure 1(e), where the effect of the heat treatment at 1000 °C is shown. Only martensitic phase appears in this case.

The anodic polarization curves obtained for the different samples and potentials in the range from the OCP to 4–5 V are shown in Figures 2–4. These curves gave an initial current increase at about 1.5 V followed by a small plateau. At a potential of about 2.7 V, the current density started to increase significantly. The effect of heat treatment on pure Ti is exemplified in Figure 2, where lower current densities for heat treatment at 1000 °C are shown. The current densities for Ti–0.2 Pd are also lower than for pure Ti (Figure 3). Both the heat treatment and the use of Pd as alloying element appear to decrease the anodic currents. Quantitative differences in the current densities of the Ti–0.2 Pd alloys were observed in the potential range from 3 to 5 V for the different heat treatments (Figure 4), the lowest current densities being found for heat treatments between 750 and 850 °C.

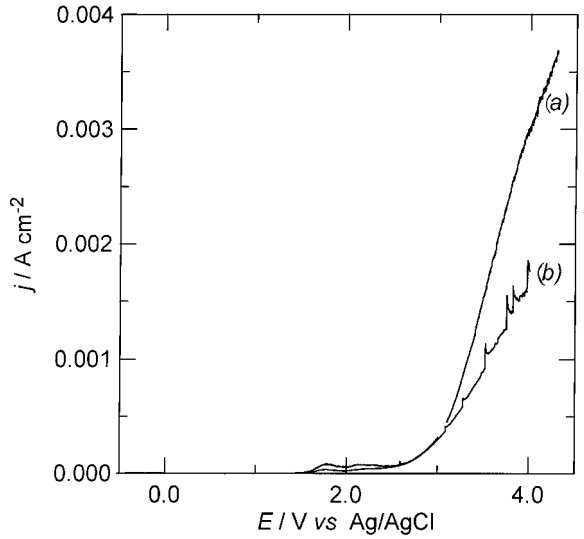

Fig. 2. Anodic polarization curves of pure Ti: (a) without heat treatment and (b) heat-treated at 1000 °C. Sweep rate 0.2 mV s^{-1}.

In the potential range 3–5 V, the j/E curves gave a maximum with peak currents lower than 3.5 mA cm^{-2}. Superposed on these maxima, a current noise was also found (e.g., the potential region between 4 and 5 V for curve (e) in Figure 4), in particular for the highest peak currents (cf. curves (a) and (e)). This current noise was due to clearly perceptible gas evolution, probably O_2 and Cl_2. The rapid current increases in curve (b) of Figure 2 and in curve (a) of Figure 4 were produced by the introduction of forced convection (vigorous stirring of the electrolyte). In this case, the current increased because the gas bubbles were more easily separated from the electrode surface. When forced convection was suppressed, the current slightly decreased to follow the initial curve.

The specimens polarized up to 4–5 V presented a patina, from yellow to violet, and no pitting was observed by SEM or optical microscopy. The surface

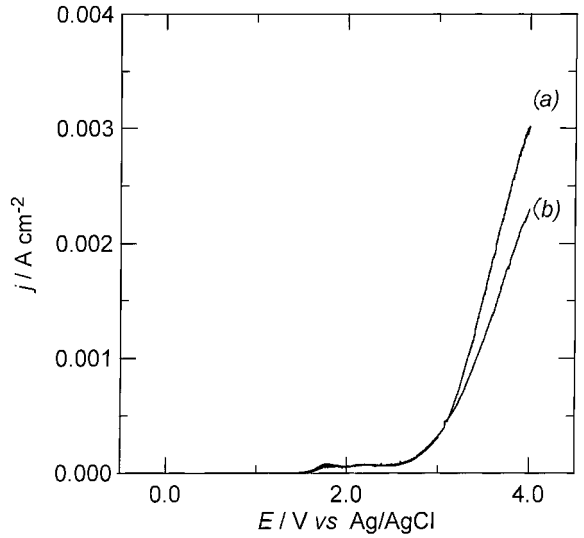

Fig. 3. Anodic polarization curves of (a) pure Ti and (b) Ti–0.2 Pd, without heat treatment. Sweep rate 0.2 mV s^{-1}.

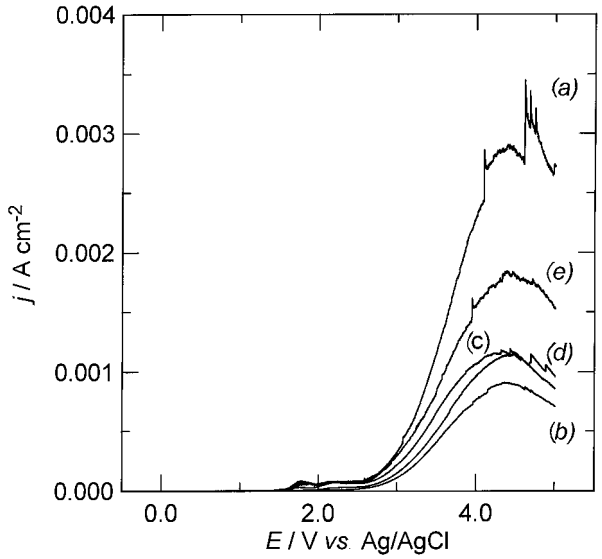

Fig. 4. Anodic polarization curves of Ti–0.2 Pd alloys: (a) without heat treatment and (b) heat-treated at 750, (c) 800, (d) 850 and (e) 1000 °C. Sweep rate 0.2 mV s^{-1}.

of the alloys appeared to be covered by an oxide layer. Therefore, the current related to the anodic peak starting at about 3 V is related to an oxide growth which has a certain conductivity to allow the solution electrolysis. The differences in the peak currents can then be ascribed to differences in conductivity of the oxide films electrogenerated. In the initial stages of the oxide growth, the coexistence of different phases appear to play a role. A SEM micrograph of the surface of the specimen heat-treated at 850 °C and oxidized up to 5 V is shown in Figure 5. The alloy surface presents a rough oxide layer and the grain structure can be clearly observed. Although the grain boundaries appear to be marked, no attack in depth was found when electrode sections were examined under the microscope.

After the anodic peaks discussed above, the anodic current significantly decreased due to the continuous growth of a protective oxide layer. An anodic polarization curve up to 9.8 V for the Ti–0.2 Pd alloy heat-

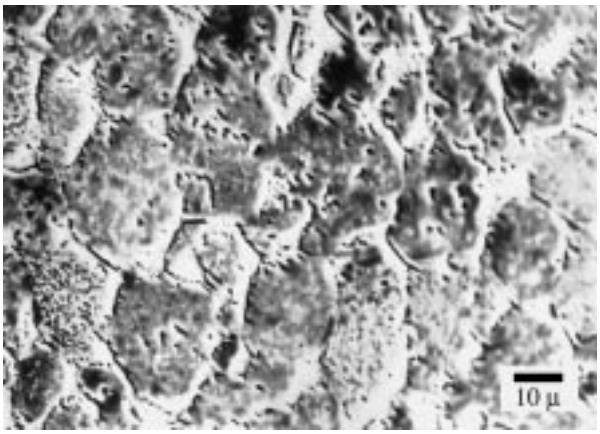

Fig. 5. SEM micrograph of Ti–0.2 Pd heat-treated at 850 °C, after oxidation up to 5 V, showing a rough oxide layer and the grain structure.

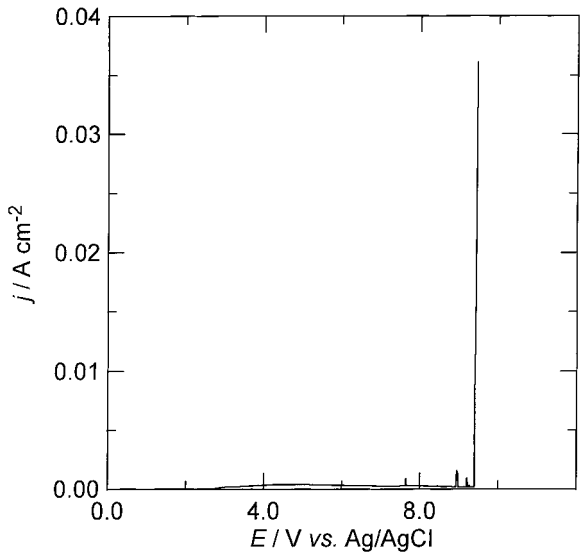

Fig. 6. Anodic polarization curve of Ti–0.2 Pd alloy heat-treated at 800 °C. Sweep rate 0.5 mV s^{-1}.

treated at 800 °C is shown in Figure 6. Although not shown in Figure 6, the current density was about 200 mA cm^{-2} at 9.5 V. The examination under the optical microscope of sections of this sample showed the presence of pitting (Figure 7). Pitting was present in the body of the sample and no crevice corrosion was observed at the metal–resin interface.

Pitting for all of the Ti–0.2 Pd alloys heat-treated at temperatures in the range 750–850 °C appeared at potentials about 10 V. No significant differences in the pitting potential were found. These values are comparable with pure titanium [5, 24]. Pitting potentials of pure Ti in chloride over 10 V were reported. Ti and Ti–0.2 Pd alloys appear to be very resistant to pitting attack in chloride. Local current densities greater than 20 A cm^{-2} were needed to sustain pitting of pure titanium in chloride at room temperature [5]. In all cases, from potentials about 8.3 V, the current presented sudden and very frequent spikes (Figure 6). This could be due to the presence of oxide film defects which were not sufficient to allow pit nucleation and propagation, and were rapidly repaired.

A SEM micrograph of the cross section of a Ti–0.2 Pd alloy heat-treated at 850 °C and submitted to an anodic polarization up to about 10 V is shown in Figure 8. Different layers parallel to the surface, marked (1) to (4), can be observed. The EDS microanalysis indicated lower oxygen content when the distance to the alloy surface increased, that is from region (1) to (4), thus showing a lower oxidation degree of the material in the same direction. Taking into account that the hardness of the alloy differs from that of the titanium oxide, the

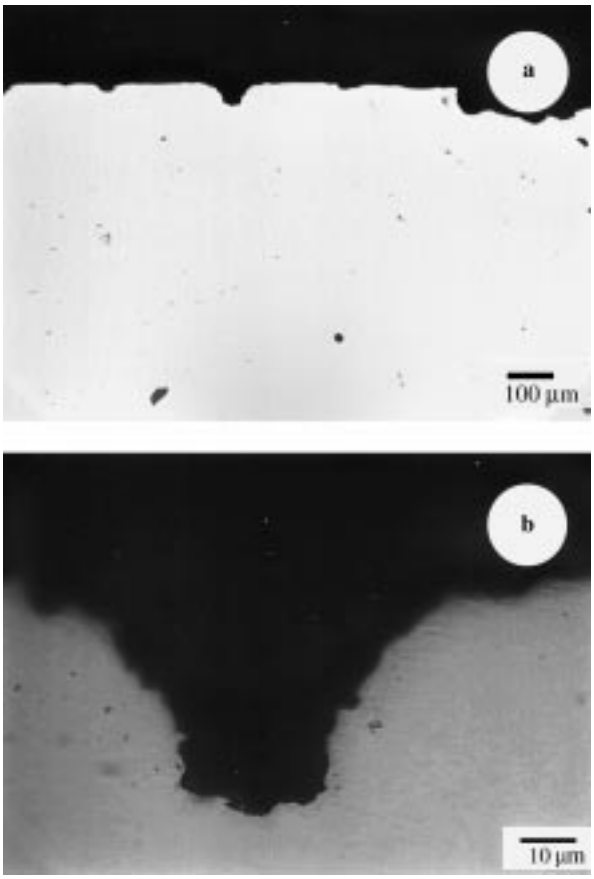

Fig. 7. Optical micrograph of a section of the Ti–0.2 Pd alloy heat-treated at 800 °C, after the anodic polarization shown in Figure 6. (a) General view of the pitted areas in the body of the sample; (b) magnification of the central pit in (a).

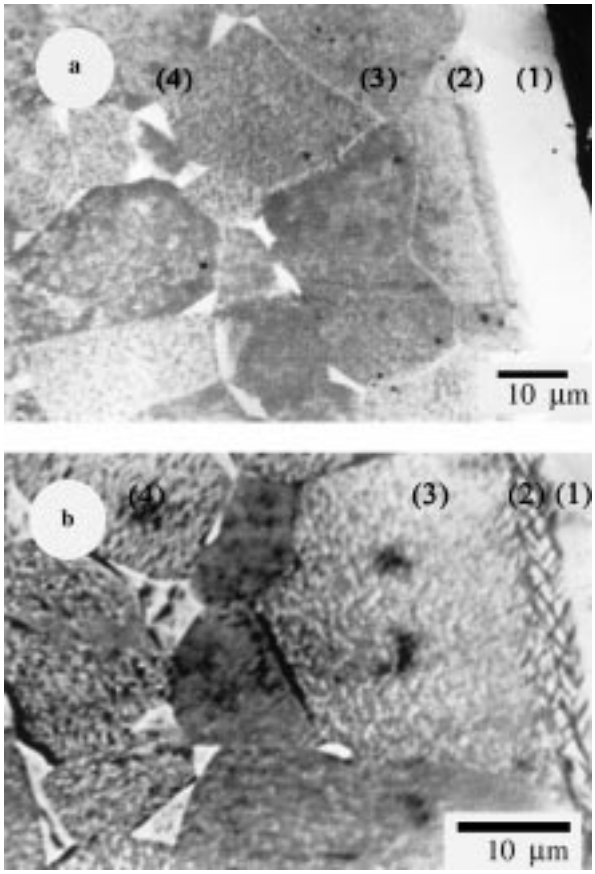

Fig. 8. SEM micrographs of a section of the Ti–0.2 Pd alloy heat-treated at 850 °C, after anodic oxidation up to about 11 V, showing (a) the morphology of the different regions and (b) a magnificated view.

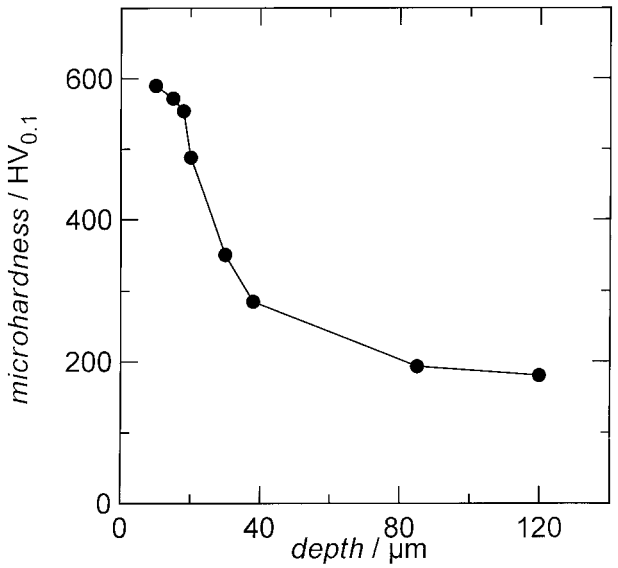

Fig. 9. Microhardness against depth for the Ti–0.2 Pd alloy heat-treated at 850 °C and anodically polarized up to about 10 V.

microhardness of the alloy was measured with depth. This plot is shown in Figure 9, in which initial microhardness values of 600 $HV_{0.1}$, corresponding to the titanium oxide, are found. The microhardness decreases as the depth increases due to concomitant decrease in the oxygen content. Region (1) corresponds to an amorphous titanium oxide film on the alloy surface and region (4) to the bulk material. As shown in Figure 8, the bulk material presents the α'-phase in the grain boundaries (white regions of the micrograph). However, no α'-phase is present in regions (1)–(3). This indicates that oxygen entering the material (as oxide) produces a great structural change, strongly affecting the intergranular martensitic phase. The structure of the external layers of the differently heat-treated Ti–0.2 Pd alloy specimens become similar upon oxidation in chloride solutions. This explains the similar behaviour of Ti and Ti–0.2 Pd alloys ahead of pitting by chloride.

4. Conclusions

Different microstructures for pure Ti and Ti–0.2 Pd alloys were obtained by heat treatment at temperatures in the range 750 to 1000 °C. Ti–0.2 Pd alloy heat-treated at temperatures in the range 750 to 850 °C presented a mixture of phases α and α', the latter being a martensitic phase produced by transformation of the β-phase during quenching. Only the α'-phase was found at 1000 °C, both for pure Ti and Ti–0.2 Pd. The anodic polarization experiments in 1% chloride solutions showed the presence of an initial plateau at about 1.5 V, an anodic peak at about 4.5 V and pitting attack at about 10 V. The anodic peak was related to the oxide film growth and to the electrolysis of the working solution. The different peak currents were explained by differences in the oxide conductivity. The measurements of the pitting corrosion potentials confirmed the passivity of Ti and Ti–0.2 Pd alloys in chloride. No effects of heat treatment on the pitting corrosion potentials of the present Ti–0.2 Pd alloys were observed. SEM observations and EDS microanalysis, together with microhardness measurements, showed that oxygen produced a great structural change in the martensitic phase. The structure of the external layers of the differently heat-treated alloy specimens studied became similar and no significant differences in their pitting potentials were found. In addition, Pd at the present concentration did not affect the behaviour of Ti ahead of pitting by chloride.

Acknowledgements

The authors acknowledge the Serveis de Microscòpia Electrònica de la Universitat Politècnica de Barcelona for the facilities in the SEM and TEM observations and the EDS microanalyses. The authors also wish to thank Mrs Marsal for her help in the microscopic analyses.

References

1. A. Michaelis, S. Kudelka and J.W. Schultze, *Electrochim. Acta* **43** (1998) 119.
2. Z.F. Wang, C.L. Briant and K.S. Kumar, *Corrosion* (NACE) **55** (1999) 128.
3. N. Casillas, S. Charlebois, W.H. Smyrl and H.S. White, *J. Electrochem. Soc.* **141** (1994) 636.
4. I. Dudgale and J.GB. Cotton, *Corros. Sci.* **4** (1964) 397.
5. T.R. Beck, *J. Electrochem. Soc.* **120** (1973) 1310.
6. T.R. Beck, *J. Electrochem. Soc.* **120** (1973) 1317.
7. A.M. Maurer, K. Merritt and S.A. Brown, *J. Biomed. Mater. Res.* **28** (1994) 241.
8. N.C. Blumenthal and V. Cosma, *J. Biomed. Mater. Res.* **23** (1989) 13.
9. D.F. Williams, *J. Medical Eng. Tech.* **1** (1977) 266.
10. M. Browne and P.J. Gregson, *Biomaterials* **11** (1994) 894.
11. T.M. Silva, J.E. Rito, A.M.P. Simões, M.G.S. Ferreira, M. da Cunha Belo and K.G. Watkins, *Electrochim. Acta* **43** (1998) 203.
12. M.A. Khan, R.L. Williams and D.F. Williams, *Biomaterials* **17** (1996) 2117.
13. L. Chen, E.-H. Chung, J.J. Williamson and K. Nobe, *Proc. Electrochem. Soc.* **97-7** (1997) 257.
14. F.J. Gil, J.A. Picas, J.M. Manero, A. Forn and J.A. Planell, *J. Alloys Comp.* **260** (1997) 147.
15. T. Watanabe and H. Naito, *J. Jpn. Inst. Met.* **52** (1988) 780.
16. M. Okada, W. Takahashi, T. Maeda, Y. Shida and T. Fakuda, *The Sumitomo Search* **44** (1990) 328.
17. ASM Committee on Ti and Ti Alloys, *in* 'Metals Handbook', Vol. 3., 9th edn (ASM, Metals Park, OH, 1980), pp. 353–360.
18. R.I. Jaffee and N. Promisel, 'The Science, Technology and Application of Titanium' (Pergamon Press, London, 1970).
19. E.W. Collings, 'The Physical Metallurgy of Titanium Alloys' (ASM, Metals Park, OH, 1984).
20. R. Gilbert and C.R. Shannon, *in* 'ASM Handbook', Vol. 4 (ASM, Metals Park, OH, 1991), pp. 913–923.
21. M.J. Donachie, 'Titanium. A Technical Guide' (ASM, Metals Park, OH, USA, 1988).
22. H. Okamoto, *J. Phase Equilibria* **14** (1993) 128.
23. M.G. Fontana and N.D. Greene, 'Corrosion Engineering', 2nd edn (McGraw-Hill, New York, 1978), pp. 334–335 and 340–342.
24. F.A. Posey and E.G. Bohlmann, *Desalination* **3** (1967) 269.